

Optical properties of two-dimensional systems of randomly distributed particles

B. N. J. Persson

*IBM Thomas J. Watson Research Center, Yorktown Heights, New York 10598
and Institut für Festkörperforschung der Kernforschungsanlage Jülich, D-5170 Jülich, West Germany*

A. Liebsch

*Institut für Festkörperforschung der Kernforschungsanlage Jülich, D-5170 Jülich, West Germany
(Received 7 July 1983)*

We have studied the optical properties of a two-dimensional system of small particles. A lattice-gas model is used to simulate nearly randomly distributed particles and the coherent-potential approximation (CPA) is applied to obtain a solution of the disorder problem. The disorder introduces characteristic structure in the absorption spectra which compares favorably with experiments.

I. INTRODUCTION

The optical properties of small-metallic-particle systems have attracted considerable interest during the last few years for several reasons. First, in the search of an effective coating for solar-energy absorbers, a promising group of materials has been found that consist of small metallic particles embedded in a dielectric host.¹ Second, it was discovered in 1974 that Raman scattering from molecules adsorbed on small silver particles is greatly enhanced (by a factor of about 10^6).² In addition, unusual behavior of small-particle systems has been predicted and observed for many thermodynamic and transport properties.³

Consider a system of small metallic particles. In an external electric field the particles will be polarized, i.e., the external field induces dipoles (and also higher multipoles). If the external field oscillates in time the radiation from the induced dipoles will generate a scattered field. The dipole moment \vec{p}_i induced in particle i at \vec{x}_i is given by

$$\vec{p}_i = \vec{\alpha}_i \cdot \vec{E}(\vec{x}_i), \quad (1)$$

where $\vec{E}(\vec{x}_i)$ is the local electric field at particle i (excluding the field from particle i) and $\vec{\alpha}_i$ its polarizability. Working in the Coulomb gauge and neglecting quadrupole and higher-multipole contributions to the local electric field, one has

$$\vec{E}(\vec{x}_i) = \vec{E}_1(\vec{x}_i) - \sum_{j(\neq i)} \vec{U}(\vec{x}_i - \vec{x}_j) \cdot \vec{p}_j, \quad (2)$$

Here $-\vec{U}(\vec{x}_i - \vec{x}_j) \cdot \vec{p}_j$ is the dipole field at particle i from particle j ,

$$\vec{U}(\vec{x}) = \frac{\vec{1}}{|\vec{x}|^3} - \frac{3\vec{x}\vec{x}}{|\vec{x}|^5},$$

and \vec{E}_1 is the transverse part of \vec{E} . Combining Eqs. (1) and (2) gives

$$\vec{p}_i = \vec{\alpha}_i \cdot \left[\vec{E}_1(\vec{x}_i) - \sum_{j(\neq i)} \vec{U}(\vec{x}_i - \vec{x}_j) \cdot \vec{p}_j \right]. \quad (3)$$

This equation is easily solved for the induced dipoles \vec{p}_i if the particles are identical and if they are localized at the sites of a cubic lattice. The result is the Clausius-Mossotti formula, or, when applied to a collection of small metallic particles, the Maxwell-Garnett (MG) formula.

Recently it was shown how to generalize the MG formula to nearly randomly distributed particles by using a lattice-gas model.⁴ That is, Eq. (3) was solved for particles located randomly on the sites of a cubic lattice. Calculations of the absorption coefficient for a system consisting of small silver particles (radius ~ 100 Å) embedded in a dielectric host (gelatin) showed good agreement with experimental results. In particular, the width of the absorption peak was correctly reproduced by this theory, while the MG formula predicted only about half of the observed width. Thus, it is important to include disorder-induced broadening in order to obtain quantitative agreement between theory and experiment.

In the present work we will consider the optical properties of a two-dimensional system of nearly randomly distributed particles. As will be seen, the effect of disorder is again very important and it gives rise to characteristic features in the absorption spectra which compare favorably with experimental observations.

A particularly important result of the present work is the fact that the disorder-induced broadening of absorption peaks is largest at relatively low particle concentrations (average spacing between neighboring particles typically a few particle radii). At these distances, multipole interactions which we have not included so far, have only minor influence on the positions and shapes of absorption lines.

This paper is sectioned as follows. In Secs. II and III we consider the optical properties of a two-dimensional system of plasma spheres arranged in an ordered lattice structure (Sec. II) and distributed nearly randomly (Sec. III). The results are discussed in Sec. IV and the conclusion is given in Sec. V. Appendix A contains a few mathematical details and Appendix B gives a short discussion of the field enhancement in surface-enhanced Raman scattering.

II. ORDERED SYSTEM OF PLASMA SPHERES

We consider first an ordered system of plasma spheres, i.e., we assume that identical plasma spheres occupy all lattice sites of a two-dimensional square Bravais lattice (lattice constant a). (This system has been treated earlier, e.g., in Ref. 5.) The polarizability of a single sphere A is⁶

$$\alpha_A(\omega) = R^3 \frac{\epsilon(\omega) - 1}{\epsilon(\omega) + 2}, \quad (4)$$

where R is the radius of the sphere and

$$\epsilon(\omega) = 1 - \frac{\omega_p^2}{\omega(\omega + i/\tau)} \quad (5)$$

is the dielectric function of the plasma. Substitution of (5) in (4) gives

$$\alpha_A(\omega) = \frac{R^3}{1 - [\omega(\omega + i/\tau)/\Omega^2]}, \quad (6)$$

where $\Omega = \omega_p/\sqrt{3}$. Thus each particle behaves as an isotropic harmonic oscillator with resonance frequency Ω and damping constant $1/\tau$.

For an ordered system, Eq. (3) can be solved by introducing collective variables,

$$\vec{p}_i = \sum_q \vec{p}_q e^{i(\vec{q} \cdot \vec{x}_i - \omega t)},$$

$$\vec{E}_i(\vec{x}_i) = \sum_q \vec{E}_i(\vec{q}) e^{i(\vec{q} \cdot \vec{x}_i - \omega t)}.$$

Inserting these expressions in (3), we obtain

$$\vec{p}_q = \alpha_A(\omega) [\vec{E}_i(\vec{q}) - \vec{U}(\vec{q}) \cdot \vec{p}_q]$$

or

$$\vec{p}_q = \frac{\alpha_A(\omega)}{1 + \alpha_A(\omega) \vec{U}(\vec{q})} \cdot \vec{E}_i(\vec{q}) \equiv \vec{\alpha}_0(\vec{q}, \omega) \cdot \vec{E}_i(\vec{q}). \quad (7)$$

We will hereafter restrict the discussion to long wavelengths, $qa \ll 1$; thus only the $\vec{q} = \vec{0}$ component of the total polarizability $\vec{\alpha}_0(\vec{q}, \omega)$ is relevant,

$$\vec{\alpha}_0(\vec{0}, \omega) = \frac{\vec{\alpha}_A(\omega)}{1 + \alpha_A(\omega) \vec{U}(0)}. \quad (8)$$

From the definition

$$\vec{U}(\vec{q}) = \sum_j' \left[\frac{\vec{1}}{|\vec{x}_j|^3} - \frac{3\vec{x}_j \vec{x}_j}{|\vec{x}_j|^5} \right] e^{i\vec{q} \cdot \vec{x}_j},$$

we get

$$\vec{U}(\vec{q} = \vec{0}) = \begin{pmatrix} -\frac{1}{2} & 0 & 0 \\ 0 & -\frac{1}{2} & 0 \\ 0 & 0 & 1 \end{pmatrix} U_0, \quad (9)$$

where

$$U_0 = \sum_j' \frac{1}{|\vec{x}_j|^3} = 9.03a^{-3}. \quad (10)$$

Since $\vec{U}(\vec{q} = \vec{0})$ is diagonal, $\vec{\alpha}_0(\vec{0}, \omega)$ may be written as

$$\vec{\alpha}_0(\vec{0}, \omega) = \begin{pmatrix} \alpha_{||}^0(\omega) & 0 & 0 \\ 0 & \alpha_{||}^0(\omega) & 0 \\ 0 & 0 & \alpha_{\perp}^0(\omega) \end{pmatrix},$$

where from (8) and (9),

$$\alpha_{||}^0(\omega) = \frac{\alpha_A(\omega)}{1 - \frac{1}{2} \alpha_A(\omega) U_0}, \quad (11)$$

$$\alpha_{\perp}^0(\omega) = \frac{\alpha_A(\omega)}{1 + \alpha_A(\omega) U_0}. \quad (12)$$

Substituting (6) into these expressions gives

$$\alpha_{||}^0(\omega) = \frac{R^3}{1 - \frac{1}{2} R^3 U_0} \frac{1}{1 - [\omega(\omega + i/\tau)/\Omega_{||}^2]}, \quad (13)$$

$$\alpha_{\perp}^0(\omega) = \frac{R^3}{1 + R^3 U_0} \frac{1}{1 - [\omega(\omega + i/\tau)/\Omega_{\perp}^2]}, \quad (14)$$

where

$$\Omega_{||}^2 = \Omega^2 (1 - \frac{1}{2} R^3 U_0),$$

$$\Omega_{\perp}^2 = \Omega^2 (1 + R^3 U_0).$$

It follows from (13) and (14) that if $1/\tau$ is small, then $\text{Im}\alpha_{||}^0(\omega)$ and $\text{Im}\alpha_{\perp}^0(\omega)$ will both be Lorentzian with the same full width at half maximum (FWHM) $1/\tau$, and centered at $\Omega_{||} < \Omega$ and $\Omega_{\perp} > \Omega$, respectively.

We must now relate the total polarizability $\vec{\alpha}_0(0, \omega)$ of the system of plasma spheres to the reflectivity r and transmission t . Consider therefore a p -polarized electromagnetic wave at an angle of incidence θ (see Fig. 1). It is possible to show that

$$r = \frac{-A(\cos^2\theta\alpha_{||}^0 - \sin^2\theta\alpha_{\perp}^0) - AB\alpha_{||}^0\alpha_{\perp}^0 e^{2i\theta}}{1 + B(\alpha_{\perp}^0 - \alpha_{||}^0) - A(\cos^2\theta\alpha_{||}^0 + \sin^2\theta\alpha_{\perp}^0) - AB\alpha_{\perp}^0\alpha_{||}^0 e^{2i\theta}}, \quad (15)$$

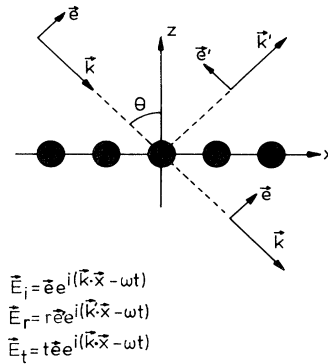


FIG. 1. Electromagnetic wave (wave vector \vec{k} , polarization vector \vec{e}) incident on a two-dimensional system of small particles gives rise to a reflected wave (\vec{k}' , \vec{e}') with amplitude r and a transmitted wave (\vec{k} , \vec{e}) with amplitude t .

$$t = \frac{1 + B(\alpha_{\perp}^0 - \alpha_{\parallel}^0)}{1 + B(\alpha_{\perp}^0 - \alpha_{\parallel}^0) - A(\cos^2\theta\alpha_{\parallel}^0 + \sin^2\theta\alpha_{\perp}^0) - AB\alpha_{\perp}^0\alpha_{\parallel}^0 e^{2i\theta}}. \quad (16)$$

Here

$$A = \frac{2\pi\omega}{ca^2} \frac{i}{\cos\theta},$$

$$B = \frac{2\pi\omega}{ca^2} \sin\theta,$$

If the terms in r and t containing A and B are much smaller than unity, then to first order in A and B ,

$$r \approx A(-\cos^2\theta\alpha_{\parallel}^0 + \sin^2\theta\alpha_{\perp}^0),$$

$$t \approx 1 + A(\cos^2\theta\alpha_{\parallel}^0 + \sin^2\theta\alpha_{\perp}^0).$$

The reflectance and transmittance are therefore

$$|r|^2 \approx 0,$$

$$|t|^2 \approx 1 + 2 \operatorname{Re}[A(\cos^2\theta\alpha_{\parallel}^0 + \sin^2\theta\alpha_{\perp}^0)],$$

and the absorbance,⁷

$$1 - |t|^2 - |r|^2 \approx -2 \operatorname{Re}[A(\cos^2\theta\alpha_{\parallel}^0 + \sin^2\theta\alpha_{\perp}^0)]$$

$$= \frac{4\pi\omega}{ca^2} \left[\cos\theta \operatorname{Im}\alpha_{\parallel}^0 + \frac{\sin^2\theta}{\cos\theta} \operatorname{Im}\alpha_{\perp}^0 \right]. \quad (17)$$

Thus, if the assumptions made in deriving this equation hold (as will be assumed hereafter), the absorption spectra will consist of two Lorentzian peaks with the same FWHM = $1/\tau$. The lower absorption peak is centered at $\Omega_{\parallel} < \Omega$ and corresponds to charge oscillations parallel to the layer of particles while the upper mode is centered at $\Omega_{\perp} > \Omega$ and corresponds to charge oscillations normal to this plane. This is illustrated in Fig. 2 where $\operatorname{Im}\alpha_{\parallel}^0(\omega)$ and $\operatorname{Im}\alpha_{\perp}^0(\omega)$ are shown for plasma spheres with radius $R = 50 \text{ \AA}$, resonance frequency $\hbar\Omega = 4 \text{ eV}$, and damping constant $\hbar\gamma = \hbar/\tau = 0.158 \text{ eV}$. The lattice constant is $a = 2R/\sqrt{0.3}$.

III. DISORDERED SYSTEM OF PLASMA SPHERES

Consider a square lattice with lattice constant $2R$. We distribute spherical particles of radius R (denoted by A)

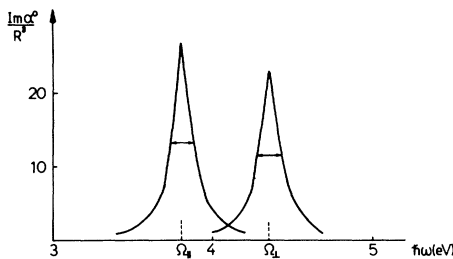


FIG. 2. $\operatorname{Im}\alpha_{\parallel}^0$ and $\operatorname{Im}\alpha_{\perp}^0$ are shown as a function of ω . In the calculation $R = 50 \text{ \AA}$, $\hbar/\tau = 0.158 \text{ eV}$, $\hbar\Omega = 4 \text{ eV}$, and $a = 2R/\sqrt{0.3}$.

randomly on the lattice points until a fraction c of the lattice points are occupied. This generates a nearly random distribution of particles with the constraint that the particles do not penetrate each other.

Figure 3(a) shows a possible configuration of particles. Physical quantities of interest, such as the polarizability of the particle system, are not those of a particular configuration but those averaged over the ensemble of all possible configurations. Within the so-called "coherent-potential approximation" (CPA), this ensemble is replaced by a periodic system with the same "ensemble-average" polarizability $\bar{\alpha}$ at each lattice site [see Fig. 3(b)]. The most important problem is to find a reasonable procedure to determine the polarizability $\bar{\alpha}$ which describes the "average" particle. According to the CPA this quantity can be self-consistently determined in the following manner: Assume that each site except the origin is occupied by the average particle and the origin by particle A (see Fig. 4). The induced dipole moment (due to a given external field) in particle A is denoted by \vec{p}_A . $\bar{\alpha}$ is then obtained by the equation

$$c \vec{p}_A = \vec{p},$$

where \vec{p} is the induced dipole moment of an average particle at the origin.

This leads to the following self-consistency condition for $\bar{\alpha}(\omega)$ ⁸:

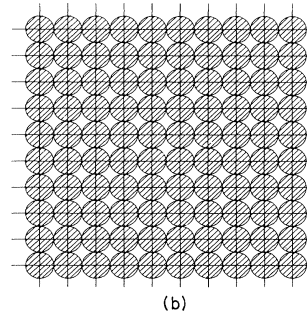
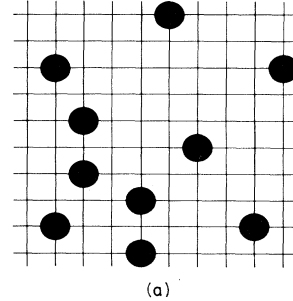


FIG. 3. (a) Possible configuration of particles generated by taking 10 numbers randomly out of 1–100. (b) In the CPA the ensemble of all possible configurations is represented by a system with an average particle at each site.

$$\vec{\alpha}(\omega) = \frac{c\vec{\alpha}_A(\omega)}{\vec{\mathbb{1}} + [\vec{\alpha}_A(\omega) - \vec{\alpha}(\omega)] \frac{1}{A^*} \int_{\text{BZ}} d^2q \{ \vec{\mathbb{U}}(\vec{q}) / [1 + \vec{\alpha}(\omega) \vec{\mathbb{U}}(\vec{q})] \}} \quad (18)$$

Here the integral is over the Brillouin zone (BZ) of area A^* . Since the average particles form a complete lattice, the total polarizability is given by Eq. (7) with α_A replaced by $\vec{\alpha}$,

$$\vec{\alpha}_0(\vec{q}, \omega) = \frac{\vec{\alpha}(\omega)}{1 + \vec{\alpha}(\omega) \vec{\mathbb{U}}(\vec{q})} \quad (19)$$

It is shown in Appendix B that Eq. (18) is satisfied by

$$\vec{\alpha} = \begin{pmatrix} \alpha_{||} & 0 & 0 \\ 0 & \alpha_{||} & 0 \\ 0 & 0 & \alpha_{\perp} \end{pmatrix}, \quad (20)$$

where $\alpha_{||}$ and α_{\perp} are given in Eqs. (A7) and (A8). Note that even if the original particles have isotropic polarizability, $\vec{\alpha}_A = \alpha_A \vec{\mathbb{1}}$, the *average* particles have only one axis of symmetry. Thus, disorder affects the $||$ and \perp modes differently.

As in the preceding section, we are only interested in the $\vec{q} = \vec{0}$ component of the total polarizability $\vec{\alpha}_0(\vec{q}, \omega)$. From Eqs. (9), (19), and (20) we get

$$\vec{\alpha}_0(0, \omega) = \begin{pmatrix} \alpha_{||}^0(\omega) & 0 & 0 \\ 0 & \alpha_{||}^0(\omega) & 0 \\ 0 & 0 & \alpha_{\perp}^0(\omega) \end{pmatrix},$$

where

$$\alpha_{||}^0(\omega) = \frac{\alpha_{||}(\omega)}{1 - \frac{1}{2} \alpha_{||}(\omega) U_0}, \quad (21)$$

$$\alpha_{\perp}^0(\omega) = \frac{\alpha_{\perp}(\omega)}{1 + \alpha_{\perp}(\omega) U_0}. \quad (22)$$

We will now present numerical results obtained from (21), (22), (A7), and (A8). Notice that (A7) and (A8) must be solved for $\alpha_{||}$ and α_{\perp} by iteration. If the zeroth-order solution is taken as $\alpha_A(\omega)$ then it turns out that about 10 iterations are necessary. Figure 5 shows $\text{Im}\alpha_{||}^0(\omega)$ and $\text{Im}\alpha_{\perp}^0(\omega)$ as a function of ω . The particles have a radius $R = 50 \text{ \AA}$ and they occupy a fraction $c = 0.3$ of the lattice sites. The resonance frequency Ω and the damping $\gamma = 1/\tau$, occurring in the expression (6) for the polarizability of a single particle, are chosen as in Fig. 2 (i.e., $\hbar\Omega = 4 \text{ eV}$ and $\hbar/\tau = 0.158 \text{ eV}$).

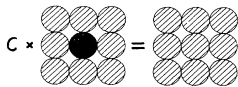


FIG. 4. Schematic representation of the equation which determines the average polarizability.

The dashed line in Fig. 5 shows the imaginary part of the polarizability of the particle system when the dipole-dipole coupling between the particles has been artificially set equal to zero. This curve is, of course, a Lorentzian centered at $\hbar\Omega = 4 \text{ eV}$ and with a FWHM = $\hbar\gamma$. As a result of the interaction between the particles, the $||$ mode is red-shifted while the \perp mode is blue-shifted, just as for the ordered-particle system studied in Sec. II.⁹ The shape and width of $\text{Im}\alpha_{||}^0(\omega)$ and $\text{Im}\alpha_{\perp}^0(\omega)$ are, however, strongly influenced by disorder. For the ordered structure these functions are both Lorentzian with the same FWHM = $\hbar\gamma$ (see Fig. 2). As Fig. 5 shows, disorder gives rise to asymmetrical peaks $\text{Im}\alpha_{\perp}^0(\omega)$ having a tail towards lower frequencies and $\text{Im}\alpha_{||}^0(\omega)$ towards higher frequencies. Moreover, both peaks are broadened, the $||$ peak being much broader than the \perp peak. This remarkable result will be discussed further below.

Figure 6 shows the variation of the width with concentration c . The broadening is seen to be largest for relatively small values of c . The average distance between neighboring particles in this range is typically 3–6 times larger than the particle radius. Thus, multipole interactions which are not included in the present calculations and which are known to be important at small interparticle spacing¹⁰ have negligible effect on the spectra shown in Fig. 5.

Figure 7 shows an experimental absorption spectrum obtained by Yamaguchi *et al.* for small silver particles located on the surface of a film of polyvinyl alcohol.⁷ The theoretical results presented above are obtained for a two-dimensional system of Drude particles located in vacuum and can therefore not be quantitatively compared with these experimental data.¹¹ For example, the “image” dipoles induced in the substrate will affect the dipole interaction between the silver particles and the “self-image interaction” will cause a red shift of both the $||$ and \perp absorption peaks.⁷ Interband transitions will also modify the absorption profile at frequencies $\hbar\omega \gtrsim 3.5 \text{ eV}$.

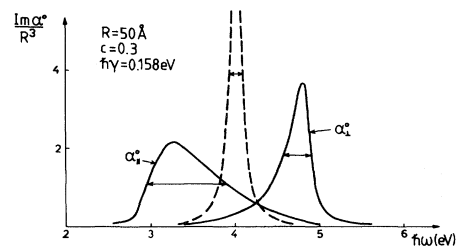


FIG. 5. Solid lines show $\text{Im}\alpha_{||}^0(\omega)$ and $\text{Im}\alpha_{\perp}^0(\omega)$. Dashed curve shows $\text{Im}[c\alpha_A(\omega)]$, i.e., the imaginary part of the total polarizability for noninteracting particles. In the calculation $R = 50 \text{ \AA}$, $c = 0.3$, $\hbar/\tau = 0.158 \text{ eV}$, and $\hbar\Omega = 4 \text{ eV}$.

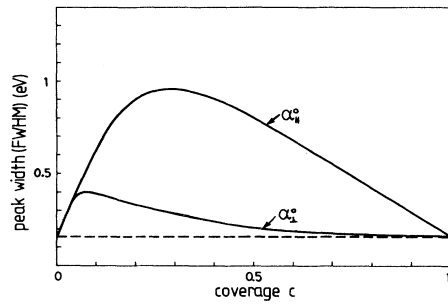


FIG. 6. FWHM of $\text{Im}\alpha_{||}^0(\omega)$ and $\text{Im}\alpha_{\perp}^0(\omega)$ as a function of the coverage c . $R = 50 \text{ \AA}$, $\hbar/\tau = 0.158 \text{ eV}$, and $\hbar\Omega = 4 \text{ eV}$.

Nevertheless, the basic disorder-induced structure predicted by the theoretical calculations is clearly visible in the experimental spectra as follows: (i) The \perp peak has a tail towards lower ω and the $||$ peak has a tail towards higher ω , and (ii) the $||$ peak is much broader than the \perp peak.

We close this section with a simple discussion of why the $||$ peak is much broader than the \perp peak. In a random distribution of particles there will be particle clusters of various sizes and shapes. Each cluster will have different resonance frequency owing to the dipole-dipole coupling between the particles. Thus there will be a distribution of absorption peaks which for an infinite system merge into a continuous absorption band. Consider now the simplest possible clusters consisting of two particles separated by a fixed distance l . For the \perp mode all such clusters will have exactly the same resonance frequency. This is not the case for the $||$ mode. Consider for example the two clusters pictured in Fig. 8. The contribution to the local electric field at particle a from particle b is $2\vec{p}/l^3$ for cluster (a) but $-\vec{p}/l^3$ for cluster (b). Thus these clusters will have rather different resonance frequencies ($\Omega[1-2(R/l)^3]^{1/2}$ and $\Omega[1+(R/l)^3]^{1/2}$, respectively). Similar differences exist in larger clusters so that as a result the distribution of resonance frequencies will be much broader for all $||$ modes than for the \perp modes.

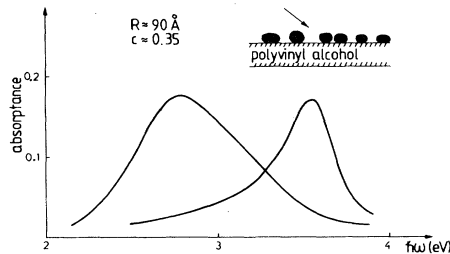


FIG. 7. Absorption spectrum of small silver particles randomly distributed on a polyvinyl alcohol sheet. Particle radius $R \approx 90 \text{ \AA}$ and coverage $c \approx 0.35$ (the uncertainty in these quantities is about 50%). By performing transmission measurement at both normal and oblique angles of incidence, it was possible to decompose the total absorbance ($\theta = 60^\circ$) into the absorbance by the $||$ and \perp modes separately. Spectrum shown is only one among several similar spectra obtained by Yamaguchi, Yoshida, and Kinbara (Ref. 7).

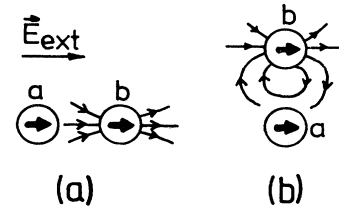


FIG. 8. Two different particle clusters. Arrows in the particles denote the induced dipoles. Clusters (a) and (b) have the resonance frequencies $\Omega[1-2(R/l)^3]^{1/2}$ and $\Omega[1+(R/l)^3]^{1/2}$, respectively, where R is the particle radius and l the distance between the centers of the particles.

IV. DISCUSSION

Real systems are certainly more complicated than the idealized model studied in Sec. III. However, the influence of disorder on the absorption spectra is best illustrated with a "clean" model calculation. Nevertheless, a quantitative comparison of the theory with experiments is meaningful only if the following points have been considered.

(a) We have neglected quadrupole and higher-multipole interactions between the particles. This is a reasonable approximation at small particle densities where the average distance between the particles is large compared with the dimensions of the particles, but it breaks down at higher particle densities.^{10,12}

(b) We have assumed that the particles are identical spheroids. In reality one will always have a distribution of particle sizes and shapes which will shift and broaden the spectral features. A good discussion of the optical properties of small particles of various shapes is given by Gersten and Nitzan in Ref. 2.

(c) We have used a Drude or free-electron-like dielectric function $\epsilon(\omega)$ for the particles. The dielectric function of a real metal has also contributions from interband transitions and from the core polarizability. Furthermore, even the Drude part of $\epsilon(\omega)$ is different for a small particle as compared with an infinite metal. For example, the relaxation time τ occurring in $\epsilon(\text{Drude})$ [see Eq. (5)] is certainly shorter for a small particle owing to the reduced electron mean-free path caused by electron collision with the surface of the particle. It has been suggested that

$$\frac{1}{\tau} = \frac{1}{\tau_{\text{bulk}}} + \frac{v_F}{R} C,$$

where v_F is the Fermi velocity and where C is a constant of order unity.¹³

(d) We have used a lattice-gas model to account for disorder. The particles were distributed on a square lattice. A better approximation would be obtained for a hexagonal lattice owing to its higher density of lattice points.⁴

(e) We have assumed that the particles are randomly distributed in space. This is certainly not always the case. Deviations from true disorder can occur due to sample preparation or due to non-negligible interactions between the particles. An illustration of the latter phenomena is a

system consisting of small helium bubbles (the "particles") in an aluminium host. If these bubbles are assumed to be randomly distributed then a very broad surface-plasmon resonance is predicted theoretically in contrast to the rather sharp resonance which is observed experimentally.¹⁴ Thus the position of the helium bubbles must be correlated in space, which has indeed been observed in electron-microscope pictures.¹⁵

V. CONCLUSION

We have presented results concerning the optical properties of two-dimensional systems of small particles. The particles are (nearly) randomly distributed in space and interact with each other through their dipole fields. The disorder is accounted for by using a lattice-gas model. The CPA was applied in order to obtain an approximate solution of the disorder problem. The disorder introduces characteristic structures in the absorption spectra which compare favorably with experimental observations.

The formalism presented in this paper can be applied to gain insight into the optical properties of many interesting and important small-particle systems, including (a) *spectroscopy of atoms and molecules adsorbed on surfaces*^{8,16}; (b) *photosynthesis*, the energy transport from the antenna chlorophylls to the active centers⁸; (c) *optical properties of rough metal surfaces*, e.g., many rough metal surfaces can be considered as consisting of a flat surface covered with randomly distributed small bumps of various sizes and shapes¹⁷ (the formalism in Sec. III is well suited to treat the optical properties of such surfaces); and (d) *surface-enhanced Raman scattering (SERS)* (see Appendix B).

ACKNOWLEDGMENTS

We would like to thank P. S. Bechthold, E. Burstein, S. Lundquist, W. Krasser, A. Otto, I. Pockrand, and P. M. Platzman for stimulating our interest in small-metallic-particle systems.

APPENDIX A

The polarizability of an average particle is given by (18),

$$\vec{\alpha} = \frac{c\vec{\alpha}_A}{\vec{\mathbb{1}} + (\vec{\alpha}_A - \vec{\alpha}) \frac{1}{A^*} \int_{\text{BZ}} d^2g \frac{\vec{\mathbb{U}}(\vec{q})}{1 + \vec{\alpha}\vec{\mathbb{U}}(\vec{q})}}, \quad (\text{A1})$$

where $\vec{\alpha}_A = \vec{\mathbb{1}}\alpha_A$ is isotropic. We will now prove that this equation is satisfied by

$$\vec{\alpha} = \begin{bmatrix} \alpha_{\parallel} & 0 & 0 \\ 0 & \alpha_{\parallel} & 0 \\ 0 & 0 & \alpha_{\perp} \end{bmatrix}. \quad (\text{A2})$$

For a square lattice $\vec{\mathbb{U}}(\vec{q})$ takes the form

$$\vec{\mathbb{U}}(\vec{q}) = \begin{bmatrix} U_{xx} & U_{xy} & 0 \\ U_{xy} & U_{yy} & 0 \\ 0 & 0 & U_{zz} \end{bmatrix}, \quad (\text{A3})$$

where U_{xx} , U_{xy} , U_{yy} , and U_{zz} are real-valued functions of \vec{q} ,

$$U_{xx} = \sum_i' \left[\frac{1}{|\vec{x}_i|^3} - \frac{3x_i^2}{|\vec{x}_i|^5} \right] \cos(\vec{q} \cdot \vec{x}_i),$$

$$U_{yy} = \sum_i' \left[\frac{1}{|\vec{x}_i|^3} - \frac{3y_i^2}{|\vec{x}_i|^5} \right] \cos(\vec{q} \cdot \vec{x}_i),$$

$$U_{xy} = \sum_i' \frac{-3x_i y_i}{|\vec{x}_i|^5} \cos(\vec{q} \cdot \vec{x}_i),$$

$$U_{zz} = \sum_i' \frac{1}{|\vec{x}_i|^3} \cos(\vec{q} \cdot \vec{x}_i).$$

Assume that (A2) is a solution to (A1). Then

$$\vec{\mathbb{1}} + \vec{\alpha} \cdot \vec{\mathbb{U}} = \begin{bmatrix} 1 + \alpha_{\parallel} U_{xx} & \alpha_{\parallel} U_{xy} & 0 \\ \alpha_{\parallel} U_{xy} & 1 + \alpha_{\parallel} U_{yy} & 0 \\ 0 & 0 & 1 + \alpha_{\perp} U_{zz} \end{bmatrix}$$

and

$$(\vec{\mathbb{1}} + \vec{\alpha} \cdot \vec{\mathbb{U}})^{-1} = \frac{1}{(1 + \alpha_{\parallel} U_{xx})(1 + \alpha_{\parallel} U_{yy}) - \alpha_{\parallel}^2 U_{xy}^2} \begin{bmatrix} 1 + \alpha_{\parallel} U_{yy} & -\alpha_{\parallel} U_{xy} & 0 \\ -\alpha_{\parallel} U_{xy} & 1 + \alpha_{\parallel} U_{xx} & 0 \\ 0 & 0 & 0 \end{bmatrix} + \frac{1}{1 + \alpha_{\perp} U_{zz}} \begin{bmatrix} 0 & 0 & 0 \\ 0 & 0 & 0 \\ 0 & 0 & 1 \end{bmatrix}. \quad (\text{A4})$$

Now consider the integral

$$\frac{1}{A^*} \int_{\text{BZ}} d^2q \vec{\alpha} \cdot \vec{\mathbb{U}} (\vec{\mathbb{1}} + \vec{\alpha} \cdot \vec{\mathbb{U}})^{-1} = 1 - \frac{1}{A^*} \int_{\text{BZ}} d^2q (\vec{\mathbb{1}} + \vec{\alpha} \cdot \vec{\mathbb{U}})^{-1}. \quad (\text{A5})$$

Since U_{xx} , U_{yy} , U_{xy}^2 , and U_{zz} are invariant under $q_x \rightarrow -q_x$ and $q_y \rightarrow -q_y$, while U_{xy} change sign under any of these substitutions, we get from (A4)

$$\frac{1}{A^*} \int_{\text{BZ}} d^2q (\vec{\mathbb{1}} + \vec{\alpha} \cdot \vec{\mathbb{U}})^{-1} = \frac{1}{A^*} \int_{\text{BZ}} d^2q \frac{1 + \frac{1}{2}\alpha_{\parallel}(U_{xx} + U_{yy})}{(1 + \alpha_{\parallel} U_{xx})(1 + \alpha_{\parallel} U_{yy}) - \alpha_{\parallel}^2 U_{xy}^2} \begin{bmatrix} 1 & 0 & 0 \\ 0 & 1 & 0 \\ 0 & 0 & 0 \end{bmatrix} + \frac{1}{A^*} \int_{\text{BZ}} d^2q \frac{1}{1 + \alpha_{\perp} U_{zz}} \begin{bmatrix} 0 & 0 & 0 \\ 0 & 0 & 0 \\ 0 & 0 & 1 \end{bmatrix}. \quad (\text{A6})$$

Here we have replaced the diagonal elements $1 + \alpha_{||} U_{yy}$ and $1 + \alpha_{||} U_{xx}$ in (A4) with $1 + \frac{1}{2}(U_{xx} + U_{yy})$ since on performing the integral over the BZ these give identical results. Substituting (A5) and (A6) into (A1) shows that (A2) is indeed a solution of (A1) if

$$\alpha_{\perp} = \frac{c\alpha_A}{1 + (\alpha_A - \alpha_{\perp}) \frac{1}{A^*} \int_{\text{BZ}} d^2q \frac{U_{zz}}{1 + \alpha_{\perp} U_{zz}}} \quad (\text{A7})$$

and

$$\alpha_{||} = \frac{c\alpha_A}{1 + (\alpha_A - \alpha_{||}) \frac{1}{A^*} \int_{\text{BZ}} d^2q \frac{\frac{1}{2}(U_{xx} + U_{yy}) + \alpha_{||}(U_{xx}U_{yy} - U_{xy}^2)}{(1 + \alpha_{||}U_{xx})(1 + \alpha_{||}U_{yy}) - \alpha_{||}^2U_{xy}^2}}$$

The last equation can be simplified slightly if we notice that $U_{xx} + U_{yy} = -U_{zz}$:

$$\alpha_{||} = \frac{c\alpha_A}{1 + (\alpha_A - \alpha_{||}) \frac{1}{A^*} \int_{\text{BZ}} d^2q \frac{-\frac{1}{2}U_{zz} + \alpha_{||}(U_{xx}U_{yy} - U_{xy}^2)}{1 - \alpha_{||}U_{zz} + \alpha_{||}^2(U_{xx}U_{yy} - U_{xy}^2)}} \quad (\text{A8})$$

Equations (A7) and (A8) are the basic equations from which the "average" polarizability $\vec{\alpha}$ is obtained by iteration. Note that α_{\perp} and $\alpha_{||}$ only depend on $\vec{U}(\vec{q})$ via the invariants (under rotations in the xy plane): U_{zz} and $U_{xx}U_{yy} - U_{xy}^2$.

Incidentally, we note here that for particles located on a three-dimensional cubic lattice, the average particle will be isotropic, i.e., $\vec{\alpha} = \alpha \vec{1}$. This result can be proved just as above and has been used in a previous paper.⁴

APPENDIX B

Many molecules adsorbed on rough silver surfaces show strongly enhanced Raman scattering. There are now both experimental and theoretical indications that this enhancement, at least in part, is caused by the large electric field set up at the surface when the resonance frequency for collective plasma oscillations in the particle system coincides with that of the external field. We will give here a rough estimate of the magnitude of this so-called "classical field enhancement."

Within the CPA all particles of the same type will have the same induced dipole moments.⁸ In the case that there is only one type of particle A of coverage c , one gets⁸

$$\vec{p}_A = \frac{1}{c} \vec{\alpha}_0 \cdot \vec{E}_1 \approx \frac{1}{c} \vec{\alpha}_0 \cdot \vec{E}_{\text{ext}}, \quad (\text{B1})$$

where the last equality is valid to zeroth order in A and B defined after Eq. (16). The electric field at the surface of a particle is

$$\vec{E}_{\text{loc}} \approx \left[\frac{3\vec{x}\vec{x}}{R^5} - \frac{\vec{1}}{R^3} \right] \cdot \vec{p}_A, \quad (\text{B2})$$

where we have neglected the contribution from the external field and from the fields of the other particles. The Raman scattering enhancement factor η is obtained from

(B1) and (B2),

$$\eta = \left| \frac{\vec{E}_{\text{loc}}}{\vec{E}_{\text{ext}}} \right|^2 = \left| (3\hat{r}\hat{r} - \vec{1}) \cdot \frac{\vec{\alpha}_0}{R^3} \cdot \vec{e} \frac{1}{c} \right|^2,$$

where $\hat{r} = \vec{x}/R$ is a unit vector along \vec{x} , and where \vec{e} is the polarization vector of \vec{E}_{ext} . Since mainly the $||$ mode is of interest in SERS [the \perp mode is centered well above typical SERS frequencies (see Fig. 7)], we put $\vec{e} = \hat{x}$ in (B3) and get

$$\eta_{||} = \frac{1}{c^2} (3 \sin^2 \theta \cos^2 \phi + 1) |\alpha_{||}^0 / R^3|^2,$$

where we have introduced spherical coordinates so that $\hat{r} \cdot \hat{x} = \sin \theta \cos \phi$. If $\langle \eta_{||}(\theta, \phi) \rangle$ denotes the angular average of $\eta_{||}(\theta, \phi)$ we get

$$\langle \eta_{||} \rangle = \frac{7}{4} \frac{1}{c^2} \left| \frac{\alpha_{||}^0}{R^3} \right|^2 \approx \frac{7}{4} \frac{1}{c^2} (\text{Im} \alpha_{||}^0 / R^3)^2.$$

From Fig. 5 we obtain $\text{Im} \alpha_{||}^0 / R^3 \approx 2$ at the $||$ peak maximum. Thus $\langle \eta_{||} \rangle \approx 10^2$. Very similar enhancement factors have been obtained by Burstein *et al.*¹⁸ and Otto¹⁹ using experimental information for $\text{Im} \alpha_{||}^0$.

Actually, not only the incident field is enhanced at the surface but so is also the Raman-scattered field. Thus the total enhancement is likely to be $10^3 - 10^4$.

The discussion above must be taken with some reservation because we have not accounted for the effect of the substrate nor for items (a)–(e) in Sec. IV. Nevertheless, it seems quite clear that the classical field enhancement alone cannot account for a total enhancement of 10^6 as observed in many SERS experiments. The enhancement factor $\sim 10^3 - 10^4$ given above is, however, consistent with an additional "chemical" enhancement of about 100, as has been indicated by some recent experiments.²⁰

- ¹A. J. Sievers, in *Solar Energy Conversion*, edited by B. O. Seraphin (Springer, Heidelberg, 1979), p. 57.
- ²See, e.g., *Surface Enhanced Raman Scattering*, edited by R. K. Chang and T. E. Furtak (Plenum, New York, 1982); A. Otto, in *Light Scattering in Solids*, edited by M. Cardona and G. Güntherodt (Springer, Berlin, 1983), Vol. IV.
- ³See the review article by H. P. Baltes and E. Simanek, in *Aerosol Microphysics II*, Vol. XX of *Topics in Current Physics*, edited by W. Marlow (Springer, Berlin, 1983).
- ⁴B. N. J. Persson and A. Liebsch, *Solid State Commun.* **44**, 1637 (1982).
- ⁵P. Clippe, R. Evrard, and A. A. Lucas, *Phys. Rev. B* **14**, 1715 (1976).
- ⁶See, e.g., J. D. Jackson, *Classical Electrodynamics* (Wiley, New York, 1975).
- ⁷T. Yamaguchi, S. Yoshida, and A. Kinbara, *Thin Solid Films* **21**, 173 (1974).
- ⁸B. N. J. Persson and R. Ryberg, *Phys. Rev. B* **24**, 6954 (1981).
- ⁹Note, however, that the shifts are much larger for the disordered system as compared with the ordered system. For example, the shifts in Fig. 2 are $\Omega_{\perp} - \Omega \approx 0.4$ and $\Omega_{\parallel} - \Omega = -0.2$ eV, while for the disordered system in Fig. 5 (which has the same particle density) $\Omega_{\perp} - \Omega \approx 0.8$ and $\Omega_{\parallel} - \Omega = -0.8$ eV, where Ω_{\perp} and Ω_{\parallel} are defined to be the frequencies where $\text{Im}\alpha_{\parallel}^0$ and $\text{Im}\alpha_{\perp}^0$ takes their maximum values.
- ¹⁰See, e.g., R. Brako, *J. Phys. C* **11**, 3345 (1978); F. Claro, *Phys. Rev. B* **25**, 7875 (1982).
- ¹¹In an interesting discussion with C. A. Murray (private communication) we have learned that it is possible to prepare systems of spherical silver particles distributed randomly (or even in a lattice-gas structure) at an SiO_2 -oil interface where the oil has the same dielectric constant as SiO_2 for frequencies in the optical region. This system would be the ideal system for testing the theoretical results presented in this work, since the influence from the dielectric host on the optical properties of the particle system is trivial.
- ¹²W. T. Doyle, *J. Appl. Phys.* **49**, 795 (1977).
- ¹³See, e.g., D. M. Wood and N. W. Ashcroft, *Phys. Rev. B* **25**, 6255 (1982), and references therein.
- ¹⁴R. Manzke and M. Campagna, *Solid State Commun.* **39**, 313 (1981).
- ¹⁵W. Jäger and J. Roth, *J. Nucl. Mater.* **93**, 756 (1980).
- ¹⁶K. Takayanagi, D. M. Kolb, K. Kambe, and G. Lehmpfuhl, *Surf. Sci.* **100**, 407 (1980).
- ¹⁷D. E. Aspnes, J. B. Theeten, and F. Hottier, *Phys. Rev. B* **20**, 3292 (1979).
- ¹⁸E. Burstein and C. Y. Chen, in *Proceedings of the Seventh International Conference on Raman Spectroscopy*, edited by W. F. Murphy (North-Holland, Amsterdam, 1980).
- ¹⁹A. Otto, in *Light Scattering in Solids*, Ref. 2, Vol. IV.
- ²⁰P. N. Sanda, J. M. Warlaumont, J. E. Demuth, J. C. Tsang, K. Christmann, and J. A. Bradley, *Phys. Rev. Lett.* **45**, 1519 (1980); J. Billmann and A. Otto, *Solid State Commun.* **44**, 105 (1982).